HELDA
HELSINGIN YLIOPISTO
HELSINGFORS UNIVERSITET
UNIVERSITY OF HELSINKI

UNIVERSITY OF HELSINKI

https://helda.helsinki.fi

Quantitative pharmacokinetic analyses of anterior and posterior elimination routes of intravitreal anti-VEGF macromolecules using published human and rabbit data

Lamminsalo, Marko

2022-09

Lamminsalo , M , Urtti , A & Ranta , V-P 2022 , ' Quantitative pharmacokinetic analyses of anterior and posterior elimination routes of intravitreal anti-VEGF macromolecules using published human and rabbit data ' , Experimental Eye Research , vol. 222 , 109162 . https://doi.org/10.1016/j.exer.20

http://hdl.handle.net/10138/355765
https://doi.org/10.1016/j.exer.2022.109162

cc_by
publishedVersion

Downloaded from Helda, University of Helsinki institutional repository.

This is an electronic reprint of the original article.

This reprint may differ from the original in pagination and typographic detail.

Please cite the original version.

Experimental Eye Research 222 (2022) 109162

Contents lists available at ScienceDirect

Experimental Eye Research

journal homepage: www.elsevier.com/locate/yexer

Research article

Quantitative pharmacokinetic analyses of anterior and posterior elimination routes of intravitreal anti-VEGF macromolecules using published human and rabbit data

Marko Lamminsalo [a,*], Arto Urtti [a,b,c], Veli-Pekka Ranta [a]

[a] School of Pharmacy, Faculty of Health Sciences, University of Eastern Finland, Kuopio, Finland
[b] Division of Pharmaceutical Biosciences, Faculty of Pharmacy, University of Helsinki, Helsinki, Finland
[c] Laboratory of Biohybrid Technologies, Institute of Chemistry, St. Petersburg State University, St. Petersburg, Russian Federation

ARTICLE INFO

Keywords:
Ocular pharmacokinetics
Intravitreal injection
Anti-VEGF macromolecule
Elimination
Pharmacokinetic modeling

ABSTRACT

The purpose of this study was to evaluate the contribution of the anterior elimination route for four anti-vascular endothelial growth factor (anti-VEGF) macromolecules (aflibercept, bevacizumab, pegaptanib and ranibizumab) after intravitreal injection using published human and rabbit data and three previously described pharmacokinetic (PK) modeling methods.

A PubMed search was used to identify published studies with concentration-time data. The data were utilized only if the intravitreally injected drugs were used as plain solutions and several criteria for a well-performed PK study were fulfilled. The three methods to analyze rabbit data were (1) the equation for vitreal elimination half-life based molecular size assuming anterior elimination, (2) Maurice equation and plot for the ratio of aqueous humor (AH) to vitreal concentration assuming anterior elimination, and (3) the equation for amount of macromolecule eliminated anteriorly based on the area under the curve in AH. The first and third methods were used for human data. In the second and third methods, AH flow rate is a key model parameter, and it was varied between 2 and 3 μl/min.

The methods were applied to data from 9 rabbit studies (1 for aflibercept, 5 for bevacizumab, and 3 for ranibizumab) and 5 human studies (1 for aflibercept, 3 for bevacizumab, and 1 for ranibizumab). Experimental half-lives of anti-VEGF macromolecules in both vitreous and aqueous humor were close to those calculated with the equations for vitreal elimination half-life in humans and rabbits. Rabbit data analyzed with Maurice plot indicated that the contribution of anterior elimination was usually at least 75%. In most human and rabbit studies, the calculated percentage of anterior elimination was at least 51%. Variability between studies was extensive for bevacizumab and ranibizumab.

The results suggest that the anterior elimination route dominates after intravitreal injection of anti-VEGF macromolecules. However, the clinical data are sparse and variability is extensive, the latter emphasizing the need of proper experimental design.

1. Introduction

Biologicals are widely used in treating diseases in the posterior segment of the eye. Intravitreal (IVT) anti-VEGF injections (aflibercept, bevacizumab, pegaptanib and ranibizumab) are the method of choice for effective retinal drug delivery in the wet form of age-related macular degeneration (AMD) and diabetic retinopathy (Maguire et al., 2016; Seguin-Greenstein et al., 2016; Sivaprasad et al., 2015; Shiragami et al., 2014). For AMD alone, the number of diseased people has been expected to increase from 196 million in 2020 to 288 million in 2040 (Wong et al.,

Abbreviations: 3D, three-dimensional; AH, aqueous humor; AMD, age-related macular degeneration; anti-VEGF, anti-vascular endothelial growth factor; A_{TM}, amount of dose eliminated anteriorly via trabecular meshwork; AUC, area under the curve; AUC_a, area under the aqueous humor curve; C_a, mean concentration of macromolecule in the aqueous humor; C_v, mean concentration of macromolecule in the vitreous; f, aqueous humor flow rate; IVT, intravitreal; k_v, vitreal elimination rate constant; NCA, noncompartmental analysis; PK, pharmacokinetic; r_H, hydrodynamic radius; $t_{1/2}$, elimination half-life; V_v, volume of vitreous.

* Corresponding author. University of Eastern Finland, School of Pharmacy, P.O. Box 1627, FI-70210, Kuopio, Finland.
E-mail address: marko.lamminsalo@uef.fi (M. Lamminsalo).

https://doi.org/10.1016/j.exer.2022.109162
Received 21 February 2022; Received in revised form 17 May 2022; Accepted 20 June 2022
Available online 26 June 2022
0014-4835/© 2022 The Authors. Published by Elsevier Ltd. This is an open access article under the CC BY license (http://creativecommons.org/licenses/by/4.0/).

2014). Hence, tens of millions of IVT injections are given annually by health care professionals (Li et al., 2020).

The behavior of biologicals after intravitreal injection can be explained using pharmacokinetic principles. The injected biologicals distribute initially to the vitreal cavity, and only to a minor extent to lens (Danysh et al., 2010) and other ocular tissues (retina, ciliary body, iris) due to their high molecular weight, steric hindrance and hydrophilicity (del Amo et al., 2017). However, the small fraction of the injected dose is capable of generating effective retinal concentrations of the anti-VEGF biologicals (del Amo and Urtti, 2015; Hutton-Smith et al., 2016).

The elimination half-lives of ocular biologicals range between 5 and 10 days in human and they are roughly half of that in rabbits (del Amo et al., 2017; Caruso et al., 2020). Elimination of intravitreally injected drug can take place anteriorly via aqueous humor drainage or posteriorly through blood-retina barrier (Maurice and Mishima, 1984). There is no direct experimental method to determine the contribution of different elimination pathways, unlike the clarification of renal and hepatic elimination routes for systemic drugs, leaving the pharmacokinetic analysis of ocular tissue concentrations of biologicals the only reasonable method.

Although there have been contradictory results about the significance of elimination routes in the literature as discussed recently in del Amo et al. (2017), quantitative data and kinetic analyses in several recent studies suggest that intravitreal biologicals are eliminated mostly via anterior route (del Amo and Urtti, 2015; Hutton-Smith et al., 2016; Caruso et al., 2020; Rimpelä et al., 2018). Diffusion of biologicals in the vitreous humor is considered to be the rate limiting step for anterior elimination after intravitreal injection (del Amo et al., 2017; Stewart, 2014). Metabolism and degradation of anti-VEGF agents in the eye are negligible (Stewart, 2014).

Several numerical pharmacokinetic methods have been applied to the eye. Noncompartmental analyses describe the drug exposure in ocular tissues in a descriptive way. Compartmental models assume that the eye consists of one or several tissue compartments which are either derived empirically from the data or are based on physiology (Caruso et al., 2020; Rimpelä et al., 2018; Missel and Sarangapani, 2019). Non-compartmental and compartmental analyses are feasible for describing ocular concentrations and estimation of pharmacokinetic parameters (clearance, apparent volume of distribution, elimination half-life). Finite element modeling, an advanced version of physiologically based modeling, accurately represents ocular structures and molecular movements in micro-scale, thereby simulating local concentration gradients within individual tissues in three dimensions (3D) (Missel, 2012; Lamminsalo et al., 2018, 2020). The core idea of the models is to provide quantitative understanding of ocular pharmacokinetics and, eventually, allow development of predictive and translatable *in silico* models to speed up drug discovery and development.

Lack of pharmacokinetic understanding and sparse human data limit the use of computational modeling in ocular drug development and clinics. While pharmacokinetic data on human eye is scarce due to ethical limits of invasive sampling, more prevalent rabbit eye data has been used to predict pharmacokinetics in the human eye (del Amo and Urtti, 2015; Bussing and Shah, 2020). Robust translation of rabbit data into the patient population requires combining biological information (e.g. anatomy and physiology) and drug properties (e.g. molecular weight, lipophilicity) with relevant clinical data that can be used to validate the model (Mager and Jusko, 2008; Mann et al., 2018).

In this study, we analyzed the anterior and posterior elimination routes of intravitreally injected anti-VEGF macromolecules with three previously described pharmacokinetic modeling methods and published human and rabbit data. This is the first time the quantitative role of elimination routes of anti-VEGF macromolecules has been studied systematically.

2. Methods

2.1. Search strategy

Literature search for most used anti-VEGF proteins (Table 1) was conducted in PubMed database in June 2021 covering the time period from January 2005 to May 2021. The search included a combination of keywords: species ("rabbit" or "human"), "intravitreal", "pharmacokinetics" and macromolecule ("aflibercept", "bevacizumab", "pegaptanib" or "ranibizumab"), e.g. rabbit AND intravitreal AND pharmacokinetics AND aflibercept. Studies with controlled release formulations (liposomal or polymeric) or modified (silicone-filled) eyes were excluded to allow analysis of pure pharmacokinetics of the macromolecule after intravitreal administration of a non-modified solution. For rabbits, only articles with both vitreous and aqueous humor (anterior chamber) concentration data were included, while for humans articles with concentration data from either vitreous or aqueous humor were included. The studies were further evaluated based on pharmacokinetic criteria (see below).

2.2. Estimation of pharmacokinetic parameters and pharmacokinetic criteria

Pharmacokinetic (PK) parameters were calculated from drug concentration data for those studies that fulfilled the criteria described in search strategy (rabbit n = 12, human n = 9). Numerical concentration values were collected from the tables or they were extracted from the pharmacokinetic graphs using WebPlotDigitizer (version 4.4, November 2020, https://automeris.io/WebPlotDigitizer). The average concentration at each time point was used. Vitreous (C_v) and aqueous humor concentrations (C_a) of the anti-VEGF biologicals were used to determine elimination half-life ($t_{1/2}$), vitreal elimination rate constant (k_v), and the area under the aqueous humor curve (AUC_a) in these tissues via non-compartmental analysis (NCA) using Phoenix 64 WinNonlin software (version 8.3.1.5014 Certara). AUC_a was calculated from time zero to infinity with linear up-log down rule. The terminal elimination phase was set to start after 3–5 days for rabbit and 5–7 days for human. During the terminal elimination phase the ratio C_a/C_v was calculated at each time point.

The following PK criteria were used for further selection of studies: 1) there must be at least three time points in the terminal elimination phase, 2) the duration of terminal elimination phase must be at least twice the estimated $t_{1/2}$, 3) the extrapolated portion of AUC_a from last time point to infinity must be less than 30% of the whole AUC_a, and 4) the highest C_a/C_v at any time point during the terminal elimination phase must be less than 3-fold compared with the lowest C_a/C_v. The first three criteria are signs for well-performed PK studies. The fourth criterion was used for rabbit data to ensure that the conditions during the terminal elimination phase were close to pseudo steady-state. Theoretically, at pseudo steady-state, $t_{1/2}$ in vitreous and aqueous humor are similar and C_a/C_v should remain constant.

Three rabbit studies and four human studies were excluded based on the selection criteria. Pharmacokinetic modeling methods were applied to nine rabbit studies and five human studies (Fig. 1).

2.3. Pharmacokinetic modeling methods

An overview of the three applied modeling methods is given in Table 2. Detailed information on each method is given below.

2.3.1. Equation for vitreal elimination half-life

Vitreal elimination half-life ($t_{1/2}$) is the most frequently used intravitreal pharmacokinetic parameter. It is defined as a ratio of primary pharmacokinetic parameters:

Table 1
Properties of commercially available biologics for treatment of age-related macular degeneration (adapted from Plyukhova et al., 2020 and Joseph et al., 2017).

Generic Name	Trade name (Company)	Year approved (FDA/EMA)	Type of molecule	Biological target	MW (kDa)	r_H (nm)[a]
Aflibercept	Eylea (Regeneron)	2011/2012	Fusion protein	VEGF-A, VEGF-B isoforms and PLGF	115	5.2
Bevacizumab	Avastin off-label (Genentech)	2004/2005	Humanized full length monoclonal antibody	VEGF-A isoforms	149	5.2
Pegaptanib	Macugen (EyeTech/Pfizer)	2004/2006	RNA aptamer	VEGF A_{165}	50	7.3
Ranibizumab	Lucentis (Genentech)	2006/2007	Humanized monoclonal antibody fragment	VEGF-A isoforms	48	2.8

Abbreviations: MW molecular weight, PLGF placental growth factor, r H hydrodynamic radius, VEGF vascular endothelial growth factor.
[a] Shatz el al. (2016), Table 1

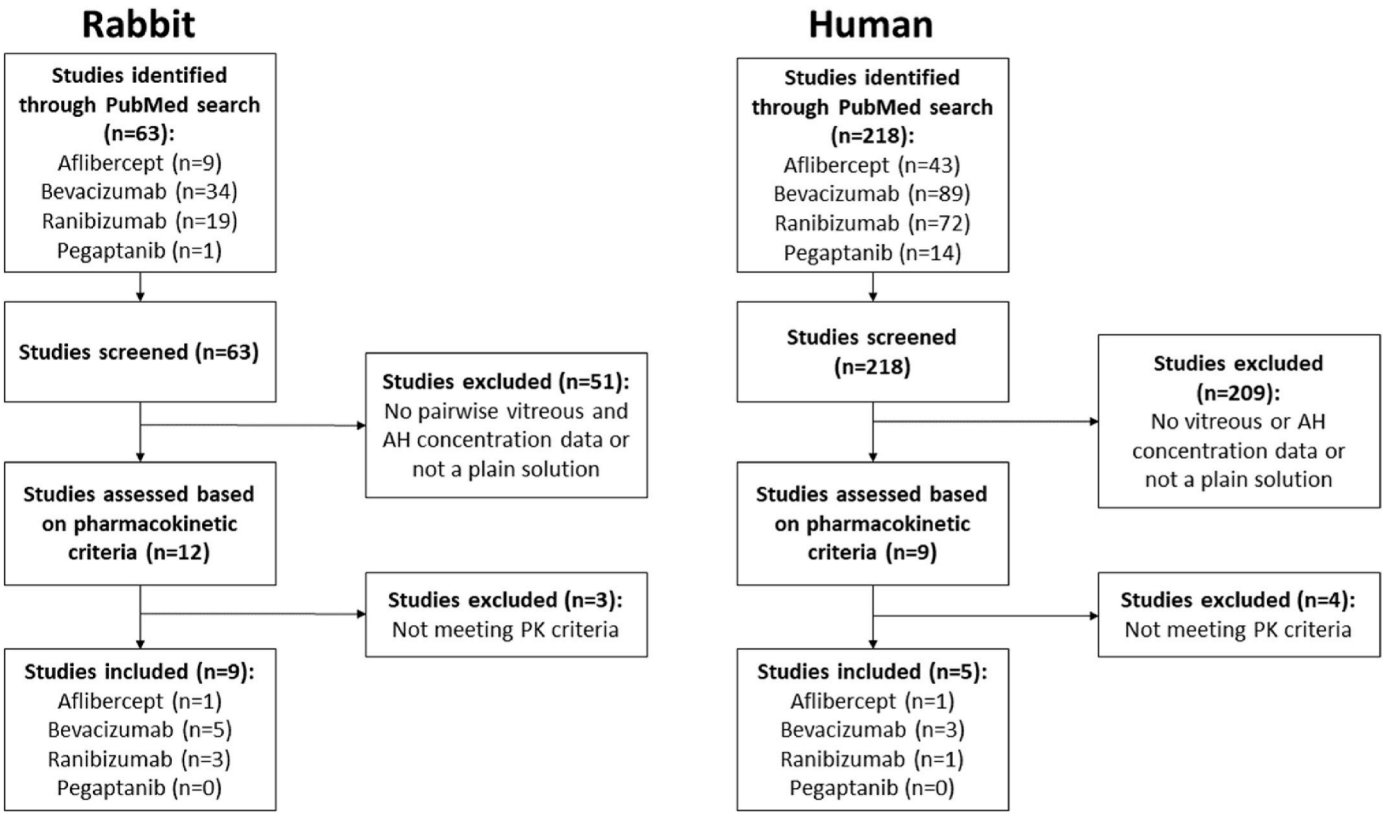

Fig. 1. Flow chart for study retrieval and selection.

$$t_{1/2} = \frac{ln2 \times V}{CL} \quad (1)$$

where V is the apparent volume of distribution and CL is the clearance from the vitreous. In the case of macromolecules, V is practically the anatomical volume of the vitreous since permeation to adjacent tissues is negligible (del Amo and Urtti, 2015). CL is a combination of anterior and posterior elimination of intact drug, since metabolism and degradation of anti-VEGF biologics in the vitreous are negligible (Stewart, 2014). Albeit useful, the half-life is a secondary pharmacokinetic parameter and thus cannot be linked directly to physiological or pathophysiological alterations in the eye.

Hutton-Smith et al. (2016) assumed that 1) the vitreous is a sphere with different volume in various species and 2) diffusion from vitreous to aqueous humor constitutes the principal pathway for intravitreal elimination of macromolecules. Furthermore, they estimated that 3) the area of the elimination pathway, the hyaloid membrane, is 23% for rabbit and 15% for human of the total sphere surface area. They also assumed that 4) the hyaloid membrane is porous and does not restrict the molecular transfer, and that 5) there is no back diffusion from aqueous humor to vitreous due to aqueous humor flow. The work of Hutton-Smith et al. was refined by Caruso et al. (2020) to allow estimation of vitreal elimination half-lives in rabbit and human eye using only the hydrodynamic radius (r_H) of the macromolecule such that

$$t_{1/2,rabbit} = 1.06 \times r_H \quad (2)$$

$$t_{1/2,human} = 1.94 \times r_H \quad (3)$$

where $t_{1/2}$ is given in days when the hydrodynamic radius r_H is given in nanometers (Caruso et al., 2020). In these equations, all macromolecules (48–150 kDa) are considered to be spherical. Equations (2) and (3) do not give a value for the percentage of anterior elimination. However, if the experimental $t_{1/2}$ is close to the calculated value, this suggests that the anterior route dominates. Experimental $t_{1/2}$ for the elimination from both the vitreous and the aqueous humor were compared with the calculated vitreal $t_{1/2}$, since at pseudo steady-state the values of $t_{1/2}$ in these tissues are equal.

Table 2
Summary of the pharmacokinetic modeling methods used to evaluate the elimination rate and route of anti-VEGF macromolecules in the rabbit and human eye.

Method (reference)	Equation	Minimum data required
Vitreal elimination half-life ($t_{1/2}$; days) (Caruso et al., 2020)	$t_{1/2.rabbit} = 1.06 \times r_H$ $t_{1/2.human} = 1.94 \times r_H$	r_H of the molecule (nm), MW between 48 and 150 kDa
Maurice equation and plot[a] (Maurice and Mishima, 1984)	$\frac{C_a}{C_v} = \frac{V_v}{f} k_v$	pairwise C_a and C_v at terminal elimination phase
Amount of drug eliminated anteriorly[a] (Lamminsalo et al., 2018)	$A_{TM} = f \times AUC_a$	complete C_a profile

Abbreviations: A_{TM} amount of dose eliminated anteriorly via trabecular meshwork (μg), AUC_a area under the aqueous humor curve (h × μg/μl), C_a drug concentration in the aqueous humor (μg/ml), C_v drug concentration in the vitreous (μg/ml), f aqueous humor flow rate (μl/h), k_v vitreous elimination rate constant (1/h), r_H hydrodynamic radius (nm), V_V volume of vitreous (μl).

[a] Theoretically, anterior chamber concentration should be used in these methods. However, in practice, aqueous humor concentrations were measured, and they were used in modeling.

2.3.2. Maurice equation and plot

David Maurice (Maurice and Mishima, 1984; Maurice, 1976) derived equation (4) for the ratio of drug concentration in the anterior chamber (C_a) to that in the vitreous (C_v) assuming that the whole intravitreal dose is eliminated via the anterior route and the clearance of the drug from the anterior chamber is equal to aqueous humor flow rate:

$$\frac{C_a}{C_v} = \frac{V_v}{f} k_v \quad (4)$$

where the ratio of vitreous volume (V_v) to aqueous humor flow rate (f) defines the theoretical slope of C_a/C_v ratio versus the observed vitreous elimination rate constant (k_v). Equation (4) is later called the Maurice equation and its graphical presentation, typically a log-log graph of C_a/C_v versus k_v, the Maurice plot. The equation is based on the assumption that C_a/C_v is determined at pseudo steady-state. This is the reason why the fourth PK criteria was applied to rabbit data (see above). For the human eye, applying Maurice plot was not possible due to lack of pairwise concentration data points for calculating C_a/C_v ratio. If the experimental C_a/C_v is close to the calculated value obtained with Maurice equation, this suggests that the anterior route dominates.

Partial anterior elimination can be described by adding a fractional coefficient to the slope, e.g., when half (0.5) of the dose is eliminated anteriorly:

$$\frac{C_a}{C_v} = 0.5 \times \frac{V_v}{f} k_v \quad (5)$$

For the rabbit eye, $V_V = 1.47$ ml (Green et al., 1957) and f = 3 μl/min (0.18 ml/h) (Barany and Kinsey, 1949) were used in most calculations. Since large circadian and age variation (1.46–2.53 μl/min) in f has been reported (Zhao et al., 2010), f of 2 μl/min was also used.

2.3.3. Equation for anterior elimination

The cumulative amount of macromolecule eliminated anteriorly via aqueous humor turnover through the trabecular meshwork (A_{TM}) can be calculated with the theoretical equation:

$$A_{TM} = f \times AUC_a \quad (6)$$

where f is the aqueous humor flow rate and AUC_a is the area under the aqueous concentration curve (Lamminsalo et al., 2018). Equation (6) is based on the assumption that the clearance of the macromolecule from the anterior chamber is equal to the aqueous humor flow. Thus, the elimination of biologicals through other anterior ocular tissues (lens, iris-ciliary body, cornea) is assumed to be negligible. Since f was not measured experimentally in the published PK studies used for the modeling, values of 2.0, 2.5 and 3.0 μl/min were used for both rabbits and humans. Previously, f = 2.4 ± 0.6 μl/min (Brubaker, 1982) and 1.27–2.48 μl/min (Nau et al., 2013) were measured for human and f = 3.0 μl/min (Barany and Kinsey, 1949) and 1.46–2.53 μl/min (Zhao et al., 2010) for rabbits. The percentage of anterior elimination *in vivo* was calculated as the percentage of A_{TM} from the intravitreal dose.

3. Results

3.1. Literature search and estimation of pharmacokinetic parameters from published studies

Twenty-one studies (rabbit n = 12, human n = 9, Table S2 in Electronic Supplementary Material) reported concentration-time profiles and the doses which were used for PK parameter estimation. Most studies (n = 260) were excluded from the analysis due to the lack of drug concentration-time profiles, or because the formulation was not a plain solution, or the eye was modified. No studies reported concentration values for pegaptanib in either rabbits or humans.

Pharmacokinetic parameters were determined for the selected 21 studies. A third of the studies (n = 7) were excluded due to not fulfilling PK selection criteria (Table S3 in Electronic Supplementary Material). The final set of 14 studies (rabbit n = 9, human n = 5) was collected according to the flow chart shown in Fig. 1. Since Meyer et al. (2011) included two acceptable concentration profiles obtained with 1.5 mg and 3.0 mg doses, and Kim et al. (2020) included only one (3.0 mg dose was included while 0.3 mg was excluded), the final set contained a total of 15 concentration profiles. Detailed information on the analyses is presented in Electronic Supplementary Material (Tables S4, S5 and S6).

3.2. Pharmacokinetic modeling methods

3.2.1. Equation for vitreal elimination half-life

The calculated vitreal elimination half-lives for aflibercept (5.5 days for rabbit; 10.1 days for humans), bevacizumab (5.5 days; 10.1 days), ranibizumab (3.0 days; 5.4 days) and pegaptanib (7.7 days; 14.2 days) were obtained using equations (2) and (3). For the rabbit, vitreal and aqueous humor half-lives obtained from the same study were usually close to each other (Fig. 2). In the rabbit, the mean vitreal half-life for bevacizumab (5.4 days) and for ranibizumab (2.7 days) were close to calculated values. Ranibizumab (48 kDa) is a smaller molecule than bevacizumab (149 kDa), and its experimental elimination half-lives in rabbits were systematically lower than those of bevacizumab. Human elimination half-lives were determined mostly from aqueous humor concentrations, and most values were close to the calculated vitreal half-lives.

3.2.2. Maurice equation and plot

Pairwise C_a/C_v data for Maurice equation and plot were available only for the rabbit. In Maurice plot, the line representing 100% anterior elimination depends on the aqueous humor formation rate (f) and vitreal volume (V_v). These were not determined in the studies from which concentration data were obtained. The effect of changing the formation rate from 3 μl/min to 2 μl/min is shown in Fig. 3. With both f values, the experimental data suggested that the anterior elimination route dominates. However, a large variability between different studies was evident for bevacizumab and ranibizumab, and one C_a/C_v value for bevacizumab was paradoxically far above the 100% line even with f of 2 μl/min.

3.2.3. Equation for anterior elimination

The contribution of anterior elimination was calculated with equation (6) using aqueous humor flow rates (f) between 2 and 3 μl/min (Table 3). There were 3–5 studies on bevacizumab in rabbit and human and on ranibizumab in rabbit, and in these cases the mean percentage of

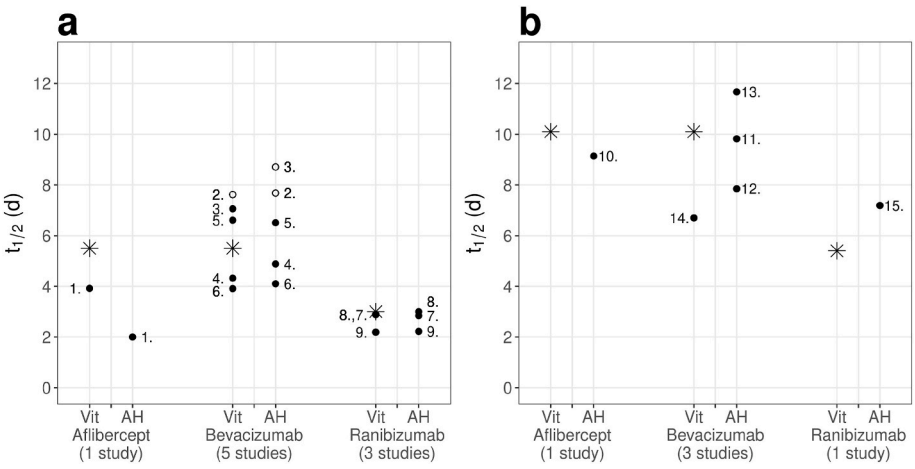

Fig. 2. Elimination half-lives of anti-VEGF macromolecules in the rabbit (a) and human eye (b). Calculated vitreal half-lives obtained with equations (2) and (3) are shown as asterisks. Reported experimental vitreal and aqueous humor elimination half-lives are shown as filled circles. When a reported value was not given, half-life was estimated from published data with noncompartmental analysis, and these values are shown as open circles. The numbers indicate the studies listed in Electronic Supplementary Table S4.

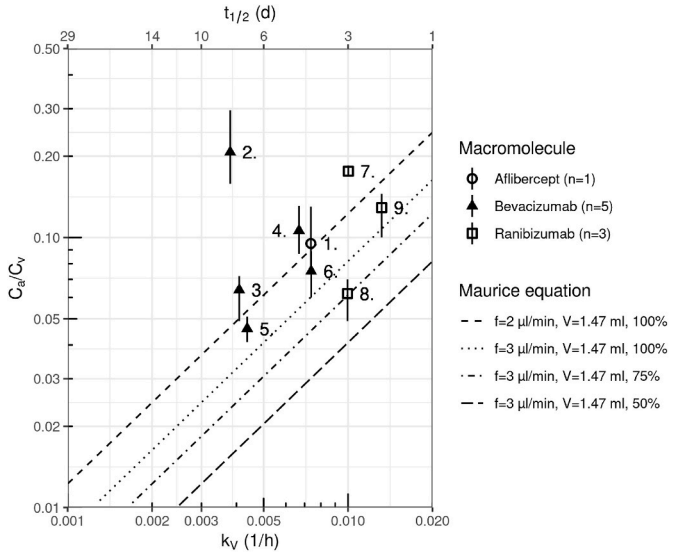

Fig. 3. Maurice plot for anti-VEGF macromolecules after intravitreal injection in the rabbit eye. The lines represent 50–100% of anterior elimination with aqueous humor formation rate of 3 µl/min and 100% anterior elimination with rate of 2 µl/min. The aqueous to vitreous concentration ratio (C_a/C_v) is shown on the vertical axis, and the elimination rate constant from vitreous (k_v) and the corresponding elimination half-life ($t_{1/2}$) on the lower and upper horizontal axis. The C_a/C_v ratio from each study is given as a line range from min to max values observed during the terminal elimination phase with the symbol presenting the average value. K_v from each study was calculated from reported $t_{1/2}$ except for one study for which k_v was estimated from published data with noncompartmental analysis since no $t_{1/2}$ value was reported. Molecules eliminating primarily anteriorly are expected to be located close to the drawn lines. The numbers indicate the studies listed in Electronic Supplementary Table S5.

anterior elimination was at least 51% with f of 2 µl/min, and at least 76% with f of 3 µl/min. However, a large between-study variability was observed. For example, the highest value for bevacizumab in rabbit was 7.6-fold compared to the lowest value. When data were available only from one study, the calculated percentage of anterior elimination was above 100% for unknown reasons. Data from individual studies are shown in Electronic Supplementary Material (Table S6).

4. Discussion

In this study, the contribution of the anterior elimination route was evaluated for anti-VEGF macromolecules after intravitreal injection using published human and rabbit data and three pharmacokinetic modeling methods. The published data were used in the modeling only if criteria for a well-performed PK study were fulfilled. The equations for vitreal half-life and Maurice equation and plot are useful for a preliminary evaluation, whereas the equation for anterior elimination gives the calculated percentage for the contribution of the anterior elimination route. Overall, our results strongly suggest that the anterior elimination route dominates. However, the clinical data are sparse and variability between studies is extensive.

Table 3
Anterior elimination (% of dose) of anti-VEGF macromolecules in the rabbit and human eye based on calculated area under the aqueous humor curve (AUC_a) and aqueous humor flow rate (f).

Species	Compound	Number of studies	Percentage of dose Mean (min–max)		
			f = 2.0 µl/min	f = 2.5 µl/min	f = 3.0 µl/min
rabbit	Aflibercept	n = 1	129	162	194
	Bevacizumab	n = 5	51 (10–76)	63 (12–95)	76 (14–114)
	Ranibizumab	n = 3	92 (63–120)	115 (79–150)	138 (95–181)
human	Aflibercept	n = 1	123	154	184
	Bevacizumab	n = 3	56 (35–90)	70 (44–113)	83 (52–136)
	Ranibizumab	n = 1	317	396	476

Experimental half-lives from the vitreous and aqueous humor were close to those calculated with equations (2) and (3) (Fig. 2). This suggests that the anterior route predominates as these equations were originally derived assuming that macromolecules are eliminated principally via the anterior route. Fig. 2 also demonstrates that in the rabbit the vitreal and aqueous humor concentrations were approximately at pseudo steady-state, because the elimination half-lives in these tissues were similar. Equations (2) and (3) are based on a recent meta-analysis of intravitreal biologicals by Caruso et al. (2020). They observed that the vitreal elimination half-life depends on the product of the hydrodynamic radius of the macromolecule and the square of the radius of the vitreal globe. Thus, the interspecies differences in elimination rate of a biologicals are mainly due to the different sizes of the vitreous, explaining the shorter $t_{1/2}$ of biologicals in rabbits than in humans (Fig. 2). Equations (2) and (3) are useful but they do not deliver definite conclusions about the major elimination route for intravitreally injected drugs.

David Maurice (1976) derived equation (4) and the plot based on it. He initially showed that C_a/C_v ratios for albumin in rabbit and hyaluronic acid in monkey were close to the line for 100% anterior elimination. Later, the rabbit data on FITC-dextrans (10, 67 and 157 kDa) by

Johnson and Maurice (1984) followed the same pattern (plotted in Lamminsalo et al., 2018). However, the location of the theoretical line for 100% anterior elimination in the plot depends on vitreous volume and aqueous humor flow rate (Fig. 3). These values are seldom determined experimentally in pharmacokinetic studies, and, therefore, literature values need to be used.

In the current study, C_a/C_v ratios for anti-VEGF macromolecules in rabbits were fairly constant during the terminal elimination phase (ratio of maximum to minimum value between 1.1 and 1.9; Electronic Supplementary Table S5 and Fig. S1) in nine acceptable data sets when the terminal elimination phase was set to start 3–5 days after the dosing. Based on experimental data and PK modeling, the peak aqueous humor concentration of intravitreally injected biologicals in rabbits usually occurs between 1–3 days (Bakri et al., 2007a, 2007b; Sinapis et al., 2011; Hutton-Smith et al., 2017; Lamminsalo et al., 2020; Caruso et al., 2020).

In our study, all C_a/C_v ratios for anti-VEGF macromolecules in rabbits were above the line for 75% anterior elimination with aqueous humor flow rate 3 μl/min (Fig. 3). However, in several studies, C_a/C_v ratios were markedly above the 100% line, and one clear outlier remained far above the 100% line even when aqueous humor flow rate was reduced to 2 μl/min. The large between-study variability for bevacizumab probably arises from both biological factors (rabbits) and experimental procedures (discussed in detail later). Tighter data can be obtained with *in vivo* fluorophotometry that Maurice used in his FITC-dextran study, since the same animals can be monitored continuously with this method, thereby minimizing biological variability. Overall, Maurice plot is a quick tool for a preliminary evaluation of anterior drug elimination if pairwise vitreal and aqueous humor concentrations are available during the terminal elimination phase at pseudo steady-state conditions.

We calculated the percentage of anterior elimination with equation (6). There were 3–5 studies on bevacizumab in rabbit and human and on ranibizumab in rabbit. In these cases, the mean percentage of anterior elimination was between 76% and 138% with aqueous humor flow rate of 3 μl/min and between 51% and 92% with aqueous humor flow rate of 2 μl/min (Table 3). For bevacizumab in rabbit, the highest value was 7.6-fold compared to the lowest value. When data were available from only one study, the percentage was always significantly above 100%. It is likely that the large variability and the paradoxical values above 100% arise partly from shortcomings in the experimental procedures in *in vivo* studies. To get meaningful results, the dose needs to be injected skillfully in the vitreous without any leakage, and the analytical assay of the biological should be accurate and precise over a very wide concentration range (e.g., initially very high concentrations in the vitreous and finally very low concentrations in the aqueous humor). Additionally, it is required that the number of time points is adequate to capture the real concentration profile in the aqueous humor. Due to the invasive nature of such experiments, many published studies report concentrations from only a few time points. Several steps concerning design of intravitreal pharmacokinetic studies have been proposed by del Amo and Urtti (2015) for obtaining reliable pharmacokinetic profiles and parameter values.

Based on our results it seems that equation (6) is the most useful approach for quantitation of anterior elimination when several studies have been performed on the same compound. In this case, the mean percentage of anterior elimination probably gives a more reliable estimate than a randomly picked individual study. The accuracy of the method could be improved by measuring the aqueous humor flow rate (f) in the PK study, thus replacing the literature value used in the calculations.

We estimated the effect of aqueous humor flow rate (f) by changing it from 3 μl/min to 1.5 μl/min in our physiologically based 3D ocular model for IgG (150 kDa) while keeping its permeability through neural retinal and combined retinal pigment epithelium-choroid constant (an unpublished simulation based on the final IgG model of Lamminsalo et al., 2020). The elimination half-life in both vitreous and aqueous humor increased from 165 h to 170 h, C_a/C_v ratio in the terminal elimination phase increased from 0.044 to 0.090, and the percentage of anterior elimination decreased from 76.1% to 75.6%, respectively. The AUC in the vitreous increased by 2.1% while the AUC in the anterior chamber increased by 106%. With f of 0.5 μl/min, the simulated half-life was 191 h, C_a/C_v ratio 0.273, and the percentage of anterior elimination 73.3%, respectively, while the vitreous AUC increased 11.9% and the anterior chamber AUC 554% compared with f of 3 μl/min. These simulations need to be verified experimentally, but they suggest the percentage of anterior elimination of biologicals is fairly insensitive to the value of f, while the anterior chamber AUC is inversely proportional to f (equation (6) when A_{TM} remains constant). Therefore, it seems that accurate PK modeling requires the determination of aqueous humor flow rate in the experimental studies.

We initially used equation (6) to check mass balance in our 3D ocular PK model (Lamminsalo et al., 2018). We also used published rabbit data on three antibodies (50–150 kDa) to show that this method gives similar percentage of anterior elimination (at least 74%; Lamminsalo et al., 2018 supplement) as obtained with the 3-compartment semi-physiological model (82–87%) (Hutton-Smith et al., 2017). Later, we obtained similar results (at least 76%) for two of these antibodies with our 3D model (Lamminsalo et al., 2020). It is important to note that our 3D ocular PK model for macromolecules and the model by Hutton-Smith et al. for macromolecules are based on the assumption that the clearance of the macromolecule from the anterior chamber is equal to aqueous humor flow rate. Therefore, equation (6) is valid for these models. In order to get the same AUC in the anterior chamber with the same aqueous humor flow rate, the same amount of macromolecule needs to be eliminated via the anterior chamber.

It should be noted that extensive anterior elimination does not imply clinical ineffectiveness. The effect of the drug is dependent on the concentration at the target site, not the quantity that is eliminated posteriorly through the retinal tissues. Therapeutic concentrations in the retina and choroid can be reached even though the posterior elimination is minimal compared to the anterior elimination (del Amo et al., 2017).

While presenting drug development tools to benefit the patient, this study may positively impact animal usage in ocular research and drug development. From a regulatory perspective, the purpose of rabbit studies is to data to demonstrate safety and efficacy at preclinical stage (Mann et al., 2018). Proper experimental design (at least four time points and two replicates per point, balanced sampling of at least two $t_{1/2}$ of the drug), in compliance with 3R (Reduce, Refine, Replace) principles to minimize animal use, results in reliable and adequate pharmacokinetic data and parameters (del Amo and Urtti, 2015; Caruso et al., 2020). Mathematical and *in silico* tools give insights into the pharmacokinetic processes, help in data interpretation and in the design of new experiments.

The presented methods are applicable also to other anti-VEGF biologicals, even though our literature search did not show relevant articles for other FDA approved clinical drugs (pegaptanib, brolicizumab). Furthermore, these tools are valid also for the kinetic analysis of other intravitreal biologicals that may be developed in the future. Moreover, anterior elimination of intravitreal drugs in special formulations cannot be analyzed with these methods, because both free and encapsulated drug should be quantitated and their profiles are affected by the release kinetics and retention of the formulation in the eye. However, the methods can be modified for considering differences in the size of vitreous globe in different species (rat, rabbit, monkey, pig, human), thereby facilitating inter-species translation during drug development (Caruso et al., 2020; Maurice and Mishima, 1984).

5. Conclusions

We analyzed the available data on intravitreal pharmacokinetics of anti-VEGF macromolecules in rabbits and humans to estimate the major

elimination route. Our results strongly suggest that the anterior elimination route dominates in the elimination of biologicals in both species. Three approaches were used to analyze the route of elimination from the vitreous. Of the published studies with concentration profiles, only two thirds fulfilled the criteria for a well-performed PK study, emphasizing the need of proper experimental design. Overall, the presented methods are useful in gaining understanding on the elimination processes of intravitreally injected biologicals.

Funding statement

The work was supported by the Academy of Finland (A.U.), Emil Aaltonen Foundation (M.L.) and Silmä- ja kudospankkisäätiö Foundation (M.L.).

Declaration of competing interest

None.

Appendix A. Supplementary data

Supplementary data to this article can be found online at https://doi.org/10.1016/j.exer.2022.109162.

References

Bakri, S.J., Snyder, M.R., Reid, J.M., Pulido, J.S., Singh, R.J., 2007a. Pharmacokinetics of intravitreal bevacizumab (Avastin). Ophthalmology 114 (5), 855–859. https://doi.org/10.1016/j.ophtha.2007.01.017.

Bakri, S.J., Snyder, M.R., Reid, J.M., Pulido, J.S., Ezzat, M.K., Singh, R.J., 2007b. Pharmacokinetics of intravitreal ranibizumab (Lucentis). Ophthalmology 114 (12), 2179–2182. https://doi.org/10.1016/j.ophtha.2007.09.012.

Barany, E., Kinsey, V.E., 1949. The rate of flow of aqueous humor; the rate of disappearance of para-aminohippuric acid, radioactive rayopake, and radioactive diodrast from the aqueous humor of rabbits. Am. J. Ophthalmol. 32, 177–188. Pt. 2 (6).

Brubaker, R.F., 1982. The flow of aqueous humor in the human eye. Trans. Am. Ophthalmol. Soc. 80, 391–474.

Bussing, D., Shah, D.K., 2020. Development of a physiologically-based pharmacokinetic model for ocular disposition of monoclonal antibodies in rabbits. J. Pharmacokinet. Pharmacodyn. 47 (6), 597–612. https://doi.org/10.1007/s10928-020-09713-0.

Caruso, A., Füth, M., Alvarez-Sánchez, R., Belli, S., Diack, C., Maass, K.F., et al., 2020. Ocular half-life of intravitreal biologics in humans and other species: meta-analysis and model-based prediction. Mol. Pharm. 17 (2), 695–709. https://doi.org/10.1021/acs.molpharmaceut.9b01191.

Danysh, B.P., Patel, T.P., Czymmek, K.J., Edwards, D.A., Wang, L., Pande, J., et al., 2010. Characterizing molecular diffusion in the lens capsule. Matrix Biol. 29 (3), 228–236. https://doi.org/10.1016/j.matbio.2009.12.004.

del Amo, E.M., Urtti, A., 2015. Rabbit as an animal model for intravitreal pharmacokinetics: clinical predictability and quality of the published data. Exp. Eye Res. 137, 111–124. https://doi.org/10.1016/j.exer.2015.05.003.

del Amo, E.M., Rimpelä, A.K., Heikkinen, E., Kari, O.K., Ramsay, E., Lajunen, T., et al., 2017. Pharmacokinetic aspects of retinal drug delivery. Prog. Retin. Eye Res. 57, 134–185. https://doi.org/10.1016/j.preteyeres.2016.12.001.

Green, H., Leopold, I.H., Sawyer, J.L., 1957. Elaboration of bicarbonate ion in intraocular fluids. II. Vitreous humor, normal values. AMA Arch Ophthalmol 57 (1), 85–89. https://doi.org/10.1001/archopht.1957.00930050093017.

Hutton-Smith, L.A., Gaffney, E.A., Byrne, H.M., Maini, P.K., Schwab, D., Mazer, N.A., 2016. A mechanistic model of the intravitreal pharmacokinetics of large molecules and the pharmacodynamic suppression of ocular vascular endothelial growth factor levels by ranibizumab in patients with neovascular age-related macular degeneration. Mol. Pharm. 13 (9), 2941–2950. https://doi.org/10.1021/acs.molpharmaceut.5b00849.

Hutton-Smith, L.A., Gaffney, E.A., Byrne, H.M., Maini, P.K., Gadkar, K., Mazer, N.A., 2017. Ocular pharmacokinetics of therapeutic antibodies given by intravitreal injection: estimation of retinal permeabilities using a 3-compartment semi-mechanistic model. Mol. Pharm. 14 (8), 2690–2696. https://doi.org/10.1021/acs.molpharmaceut.7b00164.

Johnson, F., Maurice, D., 1984. A simple method of measuring aqueous humor flow with intravitreal fluoresceinated dextrans. Exp. Eye Res. 39 (6), 791–805. https://doi.org/10.1016/0014-4835(84)90078-2.

Joseph, M., Trinh, H.M., Cholkar, K., Pal, D., Mitra, A.K., 2017. Recent perspectives on the delivery of biologics to back of the eye. Expet Opin. Drug Deliv. 14 (5), 631–645. https://doi.org/10.1080/17425247.2016.1227783.

Kim, H.M., Park, Y.J., Lee, S., Son, J.Y., Hong, H.K., Ham, M.H., et al., 2020. Intraocular pharmacokinetics of 10-fold intravitreal ranibizumab injection dose in rabbits. Transl Vis Sci Technol 9 (4), 7. https://doi.org/10.1167/tvst.9.4.7.

Lamminsalo, M., Taskinen, E., Karvinen, T., Subrizi, A., Murtomäki, L., Urtti, A., et al., 2018. Extended pharmacokinetic model of the rabbit eye for Intravitreal and Intracameral injections of macromolecules: quantitative analysis of anterior and posterior elimination pathways. Pharm. Res. (N. Y.) 35 (8), 153. https://doi.org/10.1007/s11095-018-2435-0.

Lamminsalo, M., Karvinen, T., Subrizi, A., Urtti, A., Ranta, V.-P., 2020. Extended pharmacokinetic model of the intravitreal injections of macromolecules in rabbits. Part 2: parameter estimation based on concentration dynamics in the vitreous, retina, and aqueous humor. Pharm. Res. (N. Y.) 37 (11), 226. https://doi.org/10.1007/s11095-020-02946-1.

Li, E., Donati, S., Lindsley, K.B., Krzystolik, M.G., Virgili, G., 2020. Treatment regimens for administration of anti-vascular endothelial growth factor agents for neovascular age-related macular degeneration. Cochrane Database Syst. Rev. 5 (5), CD012208. https://doi.org/10.1002/14651858.CD012208.pub2.

Mager, D.E., Jusko, W.J., 2008. Development of translational pharmacokinetic-pharmacodynamic models. Clin. Pharmacol. Ther. 83 (6), 909–912. https://doi.org/10.1038/clpt.2008.52.

Comparison of Age-related Macular Degeneration Treatments Trials (CATT) Research Group, Maguire, M.G., Martin, D.F., Ying, G.S., Jaffe, G.J., Daniel, E., et al., 2016. Five-year outcomes with anti-vascular endothelial growth factor treatment of neovascular age-related macular degeneration: the comparison of age-related macular degeneration treatments trials. Ophthalmology 123 (8), 1751–1761. https://doi.org/10.1016/j.ophtha.2016.03.045.

Mann, B.K., Stirland, D.L., Lee, H.K., Wirostko, B.M., 2018. Ocular translational science: a review of development steps and paths. Adv. Drug Deliv. Rev. 126, 195–203. https://doi.org/10.1016/j.addr.2018.01.012.

Maurice, D.M., 1976. Injection of drugs into the vitreous body. In: Leopold, I., Burns, R. (Eds.), Symposium on Ocular Therapy, vol. 9. Wiley, London, pp. 59–72.

Maurice, D.M., Mishima, S., 1984. Ocular pharmacology. In: Sears, M. (Ed.), Handbook of Experimental Pharmacology. Springer-Verlag, Berlin-Heidelberg, pp. 16–119.

Meyer, C.H., Krohne, T.U., Holz, F.G., 2011. Intraocular pharmacokinetics after a single intravitreal injection of 1.5 mg versus 3.0 mg of bevacizumab in humans. Retina 31 (9), 1877–1884. https://doi.org/10.1097/IAE.0b013e318217373c.

Missel, P.J., 2012. Simulating intravitreal injections in anatomically accurate models for rabbit, monkey, and human eyes. Pharm. Res. (N. Y.) 29 (12), 3251–3272. https://doi.org/10.1007/s11095-012-0721-9.

Missel, P.J., Sarangapani, R., 2019. Physiologically based ocular pharmacokinetic modeling using computational methods. Drug Discov. Today 24 (8), 1551–1563. https://doi.org/10.1016/j.drudis.2019.05.039.

Nau, C.B., Malihi, M., McLaren, J.W., Hodge, D.O., Sit, A.J., 2013. Circadian variation of aqueous humor dynamics in older healthy adults. Invest. Ophthalmol. Vis. Sci. 54 (12), 7623–7629. https://doi.org/10.1167/iovs.12-12690.

Plyukhova, A.A., Budzinskaya, M.V., Starostin, K.M., Rejdak, R., Bucolo, C., Reibaldi, M., et al., 2020. Comparative safety of bevacizumab, ranibizumab, and aflibercept for treatment of neovascular age-related macular degeneration (AMD): a systematic review and network meta-analysis of direct comparative studies. J. Clin. Med. 9 (5), 1522. https://doi.org/10.3390/jcm9051522.

Rimpelä, A.K., Kiiski, I., Deng, F., Kidron, H., Urtti, A., 2018. Pharmacokinetic simulations of intravitreal biologicals: aspects of drug delivery to the posterior and anterior segments. Pharmaceutics 11 (1), 9. https://doi.org/10.3390/pharmaceutics11010009.

Seguin-Greenstein, S., Lightman, S., Tomkins-Netzer, O., 2016. A meta-analysis of studies evaluating visual and anatomical outcomes in patients with treatment resistant neovascular age-related macular degeneration following switching to treatment with aflibercept. J Ophthalmol, 4095852. https://doi.org/10.1155/2016/4095852, 2016.

Shatz, W., Hass, P.E., Mathieu, M., Kim, H.S., Leach, K., Zhou, M., et al., 2016. Contribution of antibody hydrodynamic size to vitreal clearance revealed through rabbit studies using a species-matched fab. Mol. Pharm. 13 (9), 2996–3003. https://doi.org/10.1021/acs.molpharmaceut.6b00345.

Shiragami, C., Ono, A., Kobayashi, M., Manabe, S., Yamashita, A., Shiraga, F., 2014. Effect of switching therapy to pegaptanib in eyes with the persistent cases of exudative age-related macular degeneration. Medicine (Baltim.) 93 (18), e116. https://doi.org/10.1097/MD.0000000000000116.

Sinapis, C.I., Routsias, J.G., Sinapis, A.I., Sinapis, D.I., Agrogiannis, G.D., Pantopoulou, A., et al., 2011. Pharmacokinetics of intravitreal bevacizumab (Avastin®) in rabbits. Clin. Ophthalmol. 5, 697–704. https://doi.org/10.2147/OPTH.S19555.

Sivaprasad, S., Prevost, A.T., Bainbridge, J., Edwards, R.T., Hopkins, D., Kelly, J., et al., 2015. Clinical efficacy and mechanistic evaluation of aflibercept for proliferative diabetic retinopathy (acronym CLARITY): a multicentre phase IIb randomised active-controlled clinical trial. BMJ Open 5 (9), e008405. https://doi.org/10.1136/bmjopen-2015-008405.

Stewart, M.W., 2014. Pharmacokinetics, pharmacodynamics and pre-clinical characteristics of ophthalmic drugs that bind VEGF. Expet Rev. Clin. Pharmacol. 7 (2), 167–180. https://doi.org/10.1586/17512433.2014.884458.

Wong, W.L., Su, X., Li, X., Cheung, C.M., Klein, R., Cheng, C.Y., et al., 2014. Global prevalence of age-related macular degeneration and disease burden projection for 2020 and 2040: a systematic review and meta-analysis. Lancet Global Health 2 (2), e106–e116. https://doi.org/10.1016/S2214-109X(13)70145-1.

Zhao, M., Hejkal, J.J., Camras, C.B., Toris, C.B., 2010. Aqueous humor dynamics during the day and night in juvenile and adult rabbits. Invest. Ophthalmol. Vis. Sci. 51 (6), 3145–3151. https://doi.org/10.1167/iovs.09-4415.